Vol 15 No 3, March 2006
1009-1963/2006/15(03)/0552-04

Chinese Physics

© 2006 Chin. Phys. Soc.
and IOP Publishing Ltd

Near-field imaging of a square-lattice metallic photonic-crystal slab at the second band*

Feng Shuai(冯 帅), Feng Zhi-Fang(冯志芳), Ren Kun(任 坤), Ren Cheng(任 承), Li Zhi-Yuan(李志远)†, Cheng Bing-Ying(程丙英), and Zhang Dao-Zhong(张道中)

Institute of Physics, Chinese Academy of Sciences, Beijing National Laboratory for Condensed Matter Physics, Beijing 100080, *China*

(Received 10 October 2005; revised manuscript received 27 December 2005)

Imaging properties of a two-dimensional photonic crystal slab lens are investigated through the finite-difference time-domain method. In this paper, we consider the photonic crystal slab consisting of a square lattice of square metallic rods immersed in a dielectric background. Through the analysis of the equifrequency-surface contours and the field patterns of a point source placed in the vicinity of the photonic crystal slab, we find that a good-quality image can form at the frequencies in the second TM-polarized photonic band. Comparing the images formed at different frequencies, we can clearly see that an excellent-quality image is formed by the mechanisms of simultaneous action of the self-collimation effect and the negative-refraction effect.

Keywords: negative refraction, photonic crystal
PACC: 4270Q, 7820P

1. Introduction

Recently, negative refraction of electromagnetic (EM) waves has attracted a great deal of interest.[1−6] Negative refraction is the foundation for a variety of novel phenomena and potential applications. Pendry[1] predicted that a negative refractive-index material (NIM) slab could make a superlens with a resolution far beyond the diffraction limit that is inherent in the conventional far-field lens.

It was shown that negative refraction can also occur in photonic crystals (PCs), which are inhomogeneous periodic array of dielectric or metallic building blocks with a lattice constant comparable to the wavelength.[7−18] Especially, Luo *et al*[7,8] showed that all-angle negative refraction (AANR) could be achieved at the lowest band of two-dimensional (2D) square-lattice PCs and at a wavelength four times larger than the lattice constant, and as a result of this AANR, a subwavelength image could form in the near-field region of the PC slab. Li and Lin[9] showed that in addition to the negative refraction effect, other physical mechanisms such as the self-collimation effect and near-field scattering effect may play a dominant role in formation of the near-field subwavelength image. He *et al*[10] showed that the focusing properties of such a photonic crystal slab are mainly due to the negative refraction effect for large incident angles, rather than the self-collimation effect. Up to now, most discussions about the imaging properties of a square-lattice PC slab are focused on the frequencies in the lowest photonic band. In this paper, we will show that a good-quality image can also be achieved at the second TM-polarized photonic band of a PC slab consisting of a square lattice of square metallic rods immersed in a dielectric background.

2. Simulation and discussion

We consider a 2D square lattice of square metallic rods immersed in a dielectric background with the lattice constant a. When the frequency of an EM wave is much lower than the collision frequency of the electrons in a metal, the metal can be described by a frequency-independent conductivity. From Maxwell

*Project supported by the National Key Basic Research Special Foundation of China (Grant Nos 2004CB719804 and 2001CB610402), the National Natural Science Foundation of China (Grant No 10404036) and National Center for Nanoscience and Technology, China (Grant No 2003CB7169) also the support from the supercomputing Center, CNIC, CAS.

†E-mail: lizy@aphy.iphy.ac.cn

equations, the equivalent relative permittivity for the metal is $\varepsilon = 1 + \mathrm{i}\frac{\sigma}{\omega}$, which is complex and its imaginary part is proportional to ω^{-1}. Here σ is the conductivity of the metal, and ω is the angular frequency of the EM wave. In this paper, we use copper's conductivity $\sigma = 5.8 \times 10^7$ S/m, and only consider the TM polarization, where the electric field E_z is kept parallel to the extension axis of the metallic rods (assumed to be the z axis). In all the simulations, the sidelength of the square metallic rods is kept at $l = 0.3a$ with $a = 2$cm. One side of the square rods is placed along the ΓX direction (see Fig.1). The permittivity of the background material is set to be ε=18.

To investigate the possible existence of negative refraction and imaging effect in the current metallic PC structure, we should first have a full knowledge about the photonic band structures and equifrequency-surface (EFS) contours. For this purpose, we employ the finite-difference time-domain (FDTD) method[19,20] under periodic boundary conditions to calculate the band structures and EFS contours of the above PC at the TM polarization mode. The calculated band structures for the several lowest photonic bands along the high-symmetric lines in the first Brillouin zone (BZ) are shown in Fig.1(a). The dashed line represents the light line of the air environment. According to Pendry's theory, when AANR occurs, the frequency must be below this line when the EM waves transmit through the PC slab along the ΓX direction. We can see from Fig.1(a) that the metallic rods lift the first TM-polarized band and cause a stop band at the lowest frequencies. The cutoff frequency of this metallic PC is 0.118 (in units of $2\pi c/a$). A complete band gap opens between the first and second bands, and lies at frequencies 0.173–0.195. The second band spans from 0.195 to 0.243, and a partial band gap in the ΓX direction appears between the second and third bands.

Figure 1(b) shows the several calculated EFS contours in the second photonic band. We can see that most part of the 0.206 contour, which are centred around the ΓX line, are quite flat and have the surface normal pointing to the $X\Gamma$ direction. As the group velocity for a given Bloch mode characterized by $\boldsymbol{k}$ is parallel to the EFS normal at this $\boldsymbol{k}$ point, we see that the group velocities of the excited Bloch wave modes centred around the ΓX line point towards the $X\Gamma$ direction, and correspond to an apparent self-collimation effect for the PC slab, which we assume to have a surface normal parallel to the ΓX direction. In the other small part centred around the ΓM line, the curve is convex with respect to the Γ point, which means a negative refraction direction. The 0.215 contour is similar to the 0.206 one. The only difference is the region reduced where the EFS contours are flat and have the surface contour pointing to the $X\Gamma$ direction, as compared with the 0.206 contour. When the frequency becomes 0.225, almost all the contours are convex towards the Γ point.

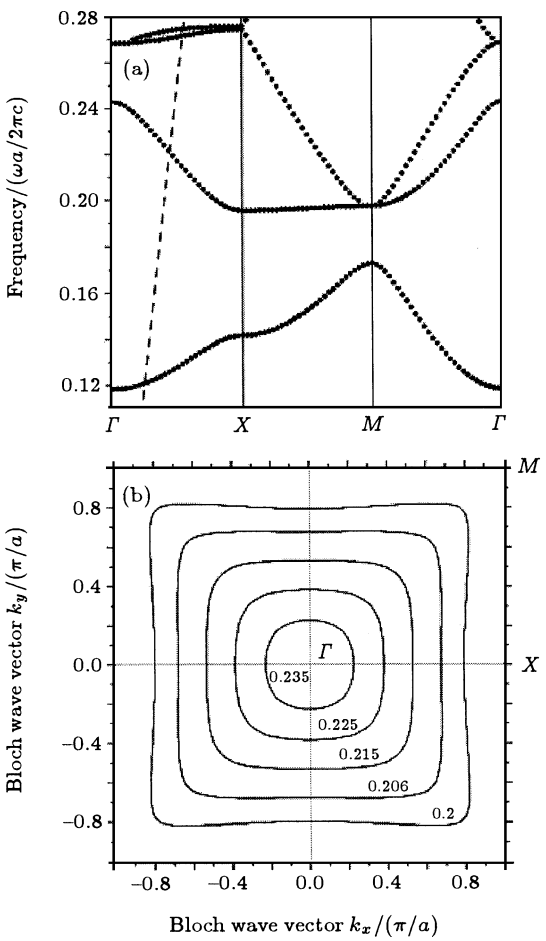


Fig.1. (a) TM band structures and (b) EFS contours of the metallic PC. The PC is composed of a square lattice of metallic rods in a dielectric background. The metal has a constant conductivity of $\sigma = 5.8\times10^7$S/m. The sidelength of the rods is $l = 0.3a$ with $a = 2$cm. The permittivity of the background material is 18. The dashed line represents the light line of the air environment.

We also employ the FDTD method with a boundary treatment of perfectly matched layers to visualize the propagation of EM waves through this kind of metallic PC slab. The rectangular metallic PC slab we consider is 51 layers wide and 6 layers thick, and the surface normal is along the ΓX direction. The whole PC slab is embedded in a homogeneous environment,

here assumed to be always the air with the refractive index 1. The distances from the four slab edges to the centre of the adjacent metallic rods are all $0.2a$. A point source of continuous waves is placed at the left side of the PC slab and fixed at x=$-0.5a, y$ =0. Here we assume that the centre of the metallic rods in the first layer is located at x =0, and the slab is symmetric with respect to y=0. When the frequencies of the continuous waves are 0.206, 0.215, and 0.225, the calculated E_Z field patterns are displayed in Figs.2(a), 2(b), and 2(c), respectively. We see from Fig.2(a) that the point source forms a visible image in the opposite side of the PC slab. This image is very close to the PC slab edge, and it looks more like half a circle in the outside of the PC slab. This image spot has a size (full size at half maximum) in the lateral direction about $1.8a$, corresponding to 0.3708λ. When the frequency becomes 0.215, an excellent-quality image appears on the right side of the PC slab shown in Fig.2(b). The centre of this image spot is located at a distance $0.8a$ from the right surface of the slab. The size of this image in the lateral direction is about $1.9a$, corresponding to 0.4085λ. Compared with the image shown in Fig.2(a), the centre of this image spot moves to the outside of the PC slab. When the frequency of the point source becomes 0.225, the calculated field pattern is shown in Fig.3(c). A visible image (although elongated in the lateral direction) forms at a distance $2.8a$ from the slab's right surface. The size of this image is about $2.8a$, corresponding to 0.63λ. The reason why this image is a distorted circle is that this frequency is a little above the light line of the air environment, so the diffraction effect degrades the quality of this image.

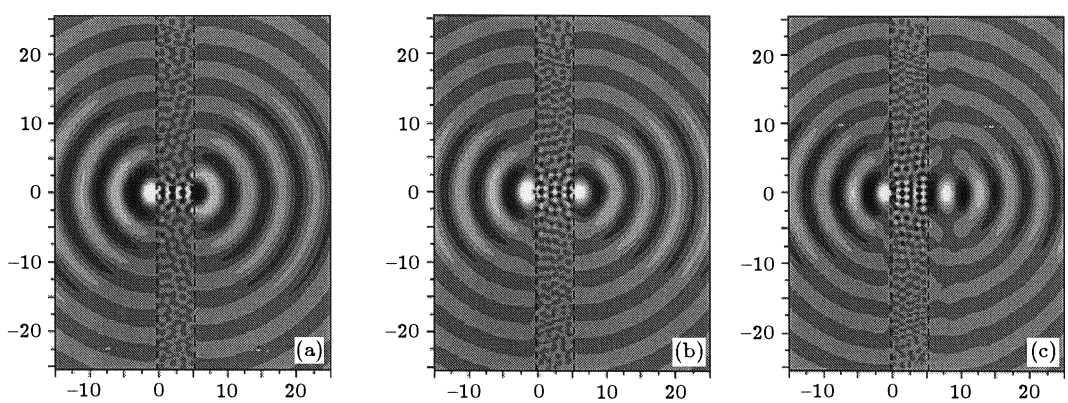


Fig.2. E_Z field patterns of a point source and its image across a metallic PC slab. The rectangular PC slab is 51 layers wide, and 6 layers thick. The slab surface normal is along the ΓX direction. The distance from the left and right slab edges to the centre of the adjacent rods is $0.2a$. The point source is placed at $x = -0.5a$, y =0, and resonant at ω=0.2 (a), 0.215 (b), 0.225 (c), $(2\pi c/a)$ respectively. The slab surfaces are represented by two dashed lines. Dark and bright regions correspond to negative and positive E_Z, respectively.

Keeping other parameters unchanged, we only alter the thickness of the PC slab, which becomes 12 layers. The corresponding field patterns are shown in Figs.3(a), 3(b), and 3(c), respectively. From Fig.3(a) we can see an apparent image spot appears on the right side of the PC slab. There is a rectangle bright channel connecting the point source and the image spot, which has a lateral size close to the source and image spot sizes. The shape of this image spot is just as the image shown in Fig.2(a). We can see from Fig.3(b) that an elongated image forms on the right side of the slab. And the width of the bright channel connecting the point source and the image spot narrows within the PC slab. The size of this image in the lateral direction is about $2.3a$, corresponding to 0.4945λ. Compared with the image shown in Fig.2(b), this image is a little elongated in the lateral direction. From Fig.3(c) we can also see an elongated image forms on the right side of the image. There appears a bright area inside the PC slab. The width of this area also narrows within the PC slab. The above calculated field patterns are consistent with the analysis of the corresponding EFS contours.

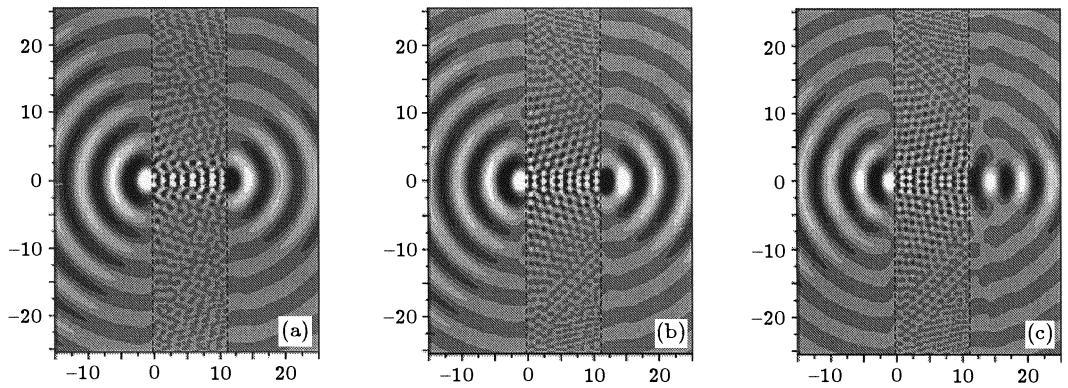


Fig.3. The same as Fig.2, except that the PC slab's thickness becomes 12 layers.

By comparing Figs.2 and 3, for the point sources with the same frequency, the distance of the image spot from the PC slab's right surface almost does not change with the slab's thickness. The PC slab thickness only influences the image quality. We know for some frequencies at the second band of the triangular-lattice PC, the EFS contours can be very nearly a perfect circle and increase inwards, meaning that the PC slab can be regarded as an effective homogeneous medium and the direction of the group velocities are opposite to that of the phase velocity, so far-field images can be formed on the opposite side of the PC slab.[11] For some frequencies in most square-lattice PC slabs, the convex degrees of the EFS contours are different for different wave vectors, so the PC cannot be regarded as a homogeneous medium at these frequencies, and only near-field image can be formed. In the above calculations, the self-collimation effect and negative refraction effect together influence the formation of the image spot, and the image quality degrades when the PC slab becomes thicker.

3. Conclusion

In conclusion, we have investigated the imaging properties of EM waves in the 2D PC slabs consisting of a square lattice of square metallic rods immersed in a dielectric background. Good-quality images can be formed in the second TM-polarized photonic band. From the analysis of the EFS contours and the corresponding field distributions at different frequencies, we can see that these images are formed by the mechanisms of the self-collimation effect and the negative refraction effect acting together. However, only near-field images can be formed for a PC slab that is not too thick. Up to now, most discussions about negative refraction are concerned with the frequencies below the light line of the air environment. Our calculated results show that even if the frequency is a little above this light line, an elongated image can also be achieved.

References

[1] Pendry J B 2000 *Phys. Rev. Lett.* **85** 3966
[2] Shelby R A, Smith D R and Schultz S 2001 *Science* **292** 77
[3] Houck A A, Brock J B and Chuang I L 2003 *Phys. Rev. Lett.* **90** 137401
[4] Smith D R and Schurig D 2003 *Phys. Rev. Lett.* **90** 077405
[5] Pacheco J, Jr., Grzegorczyk T M, Wu B I, Zhang Y and Kong J A *Phys. Rev. Lett.* **89** 257401
[6] Li J S, Zhou L, Chan C T and Sheng P 2003 *Phys. Rev. Lett.* **90** 083901
[7] Luo C Y, Johnson Steven G, Joannopoulos J D and Pendry J B 2002 *Phys. Rev.* B **65** 201104(R)
[8] Luo C Y, Johnson Steven G, Joannopoulos J D and Pendry J B 2003 *Phys. Rev.* B **68** 045115
[9] Li Z Y and Lin L L 2003 *Phys. Rev.* B **68** 245110
[10] He S L, Ruan Z C, Chen L and Shen J Q 2004 *Phys. Rev.* B **70** 115113
[11] Zhang X D 2004 *Phys. Rev.* B **70** 195110
[12] Zhang X D and Li L M 2005 *Appl. Phys. Lett.* **86** 121103
[13] Feng Z F, Zhang X D, Wang Y Q, Li Z Y, Cheng B Y and Zhang D Z 2005 *Phys. Rev. Lett.* **94** 247402
[14] Feng S , Li Z Y, Feng Z F, Cheng B Y and Zhang D Z 2005 *Phys. Rev.* B **72** 075101
[15] Feng S, Li Z Y, Feng Z F, Ren K, Cheng B Y and Zhang D Z 2005 *J. Appl. Phys.* **98** 063102
[16] Fang Y T and Shen T G 2005 *Chin. Phys. Lett.* **22** 949
[17] Wu L, Ye Z and He S L 2003 *Chin. Phys.* **12** 0642
[18] Xu X S, Wang Y Q, Han S Z, Cheng B Y and Zhang D Z 2004 *Chin. Phys.* **13** 1474
[19] Yee K S 1966 *IEEE Trans. Antenna Propag.* **14** 302
[20] Berenger J P 1994 *J. Comput. Phys.* **114** 185